Three-Dimensional Wall Jets: Axial Flow in a Stirred Tank

Kevin J. Bittorf and Suzanne M. Kresta
Dept. of Chemical and Materials Engineering, University of Alberta, Edmonton, Alberta, Canada, T6G 2G6

In this article, the flow at the wall of a stirred tank is compared with turbulent wall jet behavior. Agreement is shown to be very good. For all three axial impellers studied, the wall jet is three dimensional along the wall and baffle of the tank. The expansion of the jet is linear, and the maximum velocity decays with 1/z, where z is the dimensionless axial distance. These wall-jet characteristics help further the fundamental understanding and modeling of the bulk flow in a stirred tank and provide meaningful test data for CFD validation.

Introduction

Wall jets have been extensively examined in the literature and wall-jet theory has been well established since Glauert's solution was presented in 1956. Key characteristics of wall jets include similarity of velocity profiles, predictable decay of maximum velocity, and a linear expansion of the jet due to entrainment of surrounding fluid. In this article the characteristics of a wall jet are used to further our understanding of the flow field in stirred tanks. Other work in the literature has shown that jets can be successfully applied to model aspects of the flow in a stirred tank. The discharge from a Rushton turbine impeller can be modeled as a swirling radial jet (see review in Kresta and Wood, 1991), while a marine propellor creates a circular swirling free jet (Per et al., 1996). Along with the impeller jet, Fort (1986) suggested that there are a total of three jets in a tank stirred by an axial impeller: a swirling jet produced by the impeller; a radial wall jet at the bottom of the tank; and an annular wall jet at the walls of the tank. The objective of this work is to take these ideas further and, in particular, to examine the flow at the wall of the tank in detail. The wall jets generated by axial impellers are classified using their similarity profiles, jet decay, jet expansion, and turbulence properties. These results are compared with wall-jet theory and with other experiments.

The similarity solution for a wall jet was initially examined by Glauert (1956), who separated the similarity solution into two components: the inner (boundary) layer and the outer jet. The inner layer is treated as a boundary layer, while the similarity profile for the outer layer is modeled as a free jet. Figure 1 shows the velocity profiles for a wall jet originating at a square nozzle and flowing along the intersection of two walls. (The nomenclature for the derivation of the velocity decay and expansion is shown in this figure. There is an inner and outer layer along each of the walls.)

While the configuration in Figure 1 is similar to the geometry in a stirred tank at the intersection of the baffle and the tank wall, three-dimensional wall jets can be generated using various configurations: jets originating from orifices of various shapes and progressing along a single wall were reported by Rajaratnam and Pani (1970, 1974), Newman et al. (1972), Swamy and Bandyopadhyay (1975), and Venas et al. (1999). Baines (1985) used multiple walls. Although each of these studies had different configurations, they all found that the jet half-width (b) expands linearly and the local maximum velocity (U_m) decays inversely with the distance traveled ($U_m/U_{\text{core}} \propto 1/z$). This suggests that a three-dimensional wall jet will give consistent properties, independent of configuration, making it a good candidate for application to the complex flow in a stirred tank.

The inner layer of the wall jet has been examined extensively to determine wall friction or shear stress at the wall and the turbulent properties of the inner layer. Schwarz and Cosart (1960) report one of the first investigations of the inner layer; Launder and Rodi (1981) review the turbulent wall-jet results up to 1981; Abrahamsson et al. (1994), Eriksson et al. (1998), and Venas et al. (1999) provide more recent experimental results, and Gerodimos and So (1997) examine and review the near-wall modeling of wall jets. Most of the work cited above concentrates on the inner boundary-layer flow and the turbulent scaling of wall jets, while this study

Correspondence concerning this article should be addressed to S. M. Kresta.

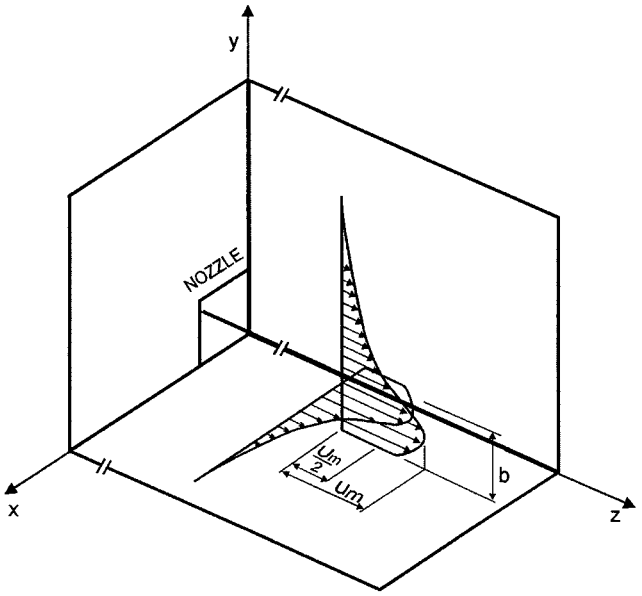

Figure 1. Three-dimensional wall jet produced by a square nozzle.

The half-width of the jet in the *y*-direction is *b*. In the tank the baffle is in the *y-z* plane and the tank wall is in the *x-z* plane.

focuses on the bulk fluid motion in the outer layer.

The outer layer of a wall jet is modeled as a free jet (Glauert, 1956; Rajaratnam, 1976; Rajaratnam and Pani, 1970, 1974). The decay of the jet is broken into three zones: a core close to the nozzle, where the velocity and turbulence are at a maximum with little decay; a characteristic decay zone, which is characteristic for the shape of the nozzle; and a radial decay zone, where the expansion of the jet is purely radial (Swamy and Bandyopadhyay, 1975). The characteristic decay zone is dependent on the experimental configuration, while the radial decay zone is general for all jets. The scaling for radial decay is easily derived from the Reynolds averaged Navier-Stokes (RANS) equations of motion. Padmanabham and Gowda (1991) provide a recent review of the decay and expansion coefficients measured for three-dimensional wall jets.

Shifting focus from the classic results for wall jets to the stirred tank, it is possible to model the flow in a stirred tank as a series of jets (Figure 2). Flow visualization shows that a discharge stream from the impeller impinges on either the wall or the bottom of the tank, depending on the impeller geometry and placement in the tank. The discharge stream from a radial impeller impinges on the wall of the tank, driving an annular wall jet [examined in detail in Bittorf (2000)]. The discharge from an axial impeller generally impinges on the bottom of the tank, driving a vertical wall jet along the intersection of the tank wall and the vertical baffle, as shown in Figure 2. In jet terminology, this is best described as a three-dimensional wall jet along two perpendicular walls originating from a theoretical point source.

In the remainder of this article the wall-jet properties are tested for application in a stirred tank. Axial velocities are measured in front of the baffle and along the wall of the

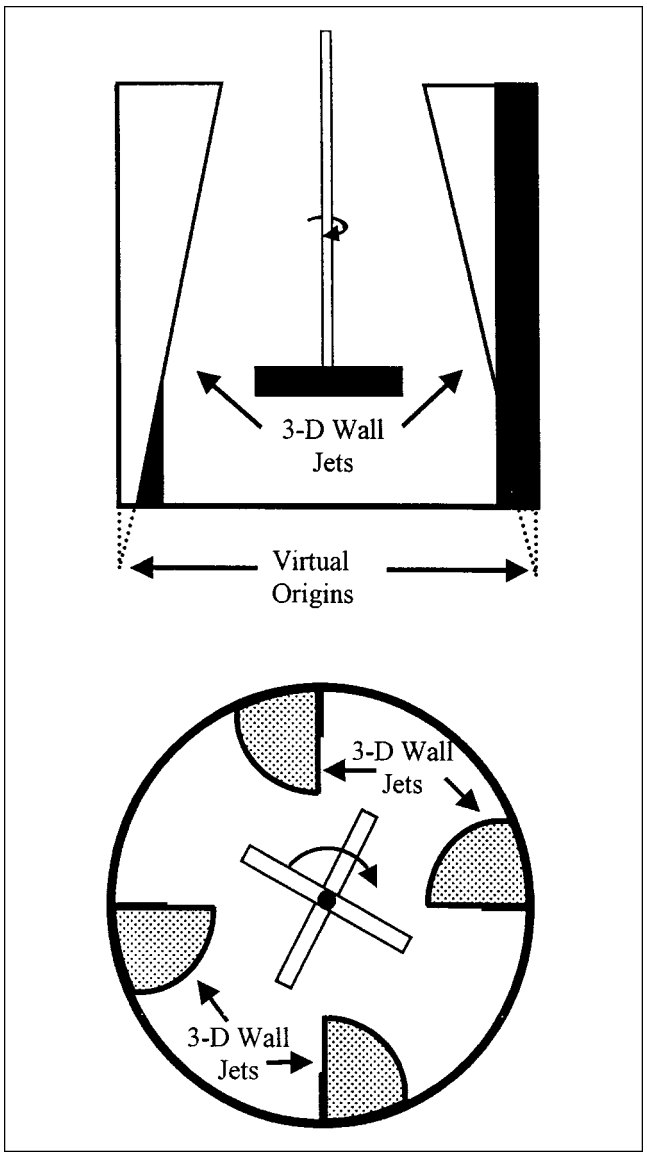

Figure 2. Location of virtual origins for a 3-D wall jet driven by an axial impeller.

The virtual origins are located approximately one baffle width below the tank.

tank. The velocity decay, jet expansion, virtual origin, and turbulent properties of the jet are compared to values predicted by theory, and to values found in the literature. As a basis for this comparison, the pertinent equations are addressed in the next section.

Theory

A three-dimensional wall jet along two perpendicular walls issuing from a square nozzle is shown in Figure 1. Only a summary of the derivation of the expansion and decay is given here, as details are available elsewhere (Rajaratnam, 1976; Rajaratnam and Pani, 1970, 1974).

The Navier-Stokes equations in rectangular coordinates are reduced using the following assumptions:

- The flow field is fully turbulent; hence, the viscous shear stress is much smaller than the turbulent shear stress.
- Body forces are balanced by static pressure.
- The boundary layer approximations are: the length scale in the x- and y-directions is much smaller than the length scale in the direction of flow, hence, $\partial/\partial x \cong \partial/\partial y \gg \partial/\partial z$; the velocity in the direction of flow is much larger than the velocity in the perpendicular direction, hence, $v \cong w \ll u$.

Given these assumptions, the Navier-Stokes equations reduce to

$$U\frac{\partial U}{\partial z} + V\frac{\partial U}{\partial y} + W\frac{\partial U}{\partial x} = -\left[\frac{\partial \overline{u'v'}}{\partial y} + \frac{\partial \overline{u'w'}}{\partial x}\right]. \qquad (1)$$

The v (or w) component of the equation reduces to show that the dynamic pressure gradient is balanced by the Reynolds stress. From this point a variety of dimensionless distance, velocity, and shear-stress variables are used to determine the similarity solution (see Rajaratnam, 1976; Rajaratnam and Pani, 1970, 1974). The solution found from the dimensionless form of Eq. 1 is

$$U_m \propto z^p \qquad b \propto z^q. \qquad (2)$$

The other equation required to solve for the exponents p and q, is the integral momentum constraint. At any point in the jet the momentum must remain constant:

$$\frac{d}{dz}\rho\int_{-\infty}^{\infty}\int_{-\infty}^{\infty} U^2\, dy\, dx = 0. \qquad (3)$$

From this equation, the variables p and q are solved. Based on the derivation by Rajaratnam (1976) and Rajaratnam and Pani (1970, 1974), the expansion and decay rates for a three-dimensional wall jet along two perpendicular walls are: velocity decay:

$$\frac{u_m}{U_{\text{nozzle}}} \propto \frac{1}{z/d_{\text{nozzle}}}, \qquad (4a)$$

jet expansion:

$$\frac{b}{d_{\text{nozzle}}} \propto \frac{z}{d_{\text{nozzle}}}, \qquad (4b)$$

where U_m is the local maximum velocity (a function of z U_{nozzle} is the core velocity of the jet (the global maximum at the nozzle outlet), b is the half-width of the jet; d_{nozzle} is the diameter of the nozzle, and z is the distance the jet has traveled.

The equations for the wall jet are now placed in the context of a stirred tank. The three major zones (core, characteristic, and radial decay) are defined as follows. The potential core is where the wall jet initially develops, and in this region, the velocities have little decay. In the case of a stirred tank, the potential core is the region close to the bottom of the tank, where the vertical flow develops. The core velocity is defined as the global maximum velocity in the jet. The characteristic decay region is where the decay exponent depends on the tank configuration. The region of radial decay is where the maximum velocity decays according to Eq. 4, independent of impeller geometry and placement in the tank.

In the wall-jet equations, the nozzle diameter is used to make the cross stream and streamwise directions dimensionless. Since there is no nozzle in a stirred tank, the tank diameter (T) is used as the characteristic length scale. Other possible length scales, the impeller diameter and the baffle width, were discarded. The experiments showed no dependence of the jet width on the impeller size, so D is not the characteristic length scale. While the baffle width may be an equally valid length scale, in these experiments the baffles are a constant fraction of T, so the tank diameter and the baffle width are indistinguishable as length scales. For the characteristic velocity, the wall-jet equations use the nozzle velocity for U_{core}. In the stirred tank, there is no nozzle and the local maximum axial velocity in the jet may increase from its initial value at the bottom of the tank as the vertical circulation is incorporated into the jet. As a result, U_{core} for the stirred tank is defined as the global maximum axial velocity in the wall jet. The resulting dimensionless jet equations for an axial impeller are:

$$\frac{U_m}{U_{\text{core}}} \propto \frac{1}{z/T} \qquad \frac{b}{T} \propto \frac{z}{T} \qquad \eta = \frac{y}{b}. \qquad (5)$$

Here U_m is the local maximum velocity at a fixed height z, z is the axial distance from the bottom of the tank, y is the distance from the tank wall, b is the position where the velocity is equal to half of the local maximum velocity, and η is the dimensionless distance from the wall.

Experimental Conditions

Experiments were designed to measure the decay and expansion of wall jets in a stirred tank. Axial velocities were measured using a laser doppler velocimeter (LDV) as described in Bittorf and Kresta (2000) and Zhou and Kresta (1996). The system parameters are summarized in Table 1. A transparent 240-mm cylindrical stirred tank enclosed in a square tank was agitated using three different impellers: a 4-bladed 45° pitched-blade turbine (PBT), a Chemineer HE-3

Table 1. Equipment Specifications

Argon laser	Output power = 300 mW Beam separation = 0.0340 m Focal length = 500 mm Wavelength of light = 514.5 nm Bragg cell frequency shift = 40 MHz Fringe spacing = 7.6 μm Velocity variability = $\pm$5%
Horizontal traverses	Computer controlled Accuracy = $\pm$0.25 mm
Vertical traverse	Manual Accuracy = $\pm$1.0 mm
Off-bottom clearance adjustment	Manual Accuracy = $\pm$0.5 mm
Seeding	In tap water—naturally occurring 1-μm particulate

Table 2. Experiments Completed

Impeller	Dia. (D/T)	Re	Clearance (C/D)	Dimensionless Core Velocity (U_{core}/V_{tip})
A310	0.58	6.53×10^4	0.32	0.290
		1.96×10^5	0.50	0.255
			0.68	0.230
HE-3	0.50	6.00×10^4	0.50	0.226
		2.40×10^5	0.67	0.210
PBT	0.33	5.33×10^4	0.40	0.326
		1.07×10^5	1.0	0.298

(HE-3), and Lightnin A310 (A310), all of standard geometry. The impeller diameter, the rotational speed, and the off-bottom clearance were varied. Water was used as the test fluid in all experiments. A complete list of experiments is given in Table 2. A cross section of the tank is shown in Figure 3a, and the measurement locations are shown in Figure 3b. Note that the $z = 0$ position is at the bottom of the tank.

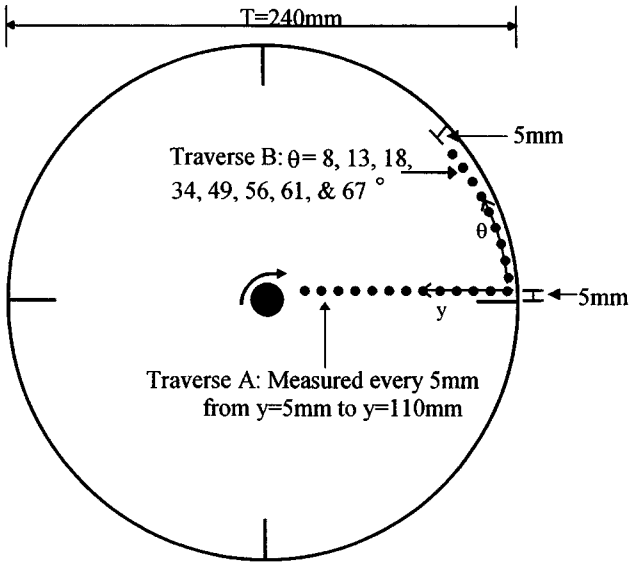

Figure 3b. Position of measurements (top view).

Results

The application of jet theory to a stirred tank may result in significant mismatch due to the effects of tank curvature, the finite width of the baffle, and the low-frequency disturbances that have been reported as ''surface welling at the baffle'' (Bruha et al., 1995) and ''macroinstabilities'' (Roussinova et al., 2000). In spite of these aspects of the flow, experimental results in this section show that the three-dimensional wall jet generated by an axial impeller follows theory very closely. Two criteria are used to assess the validity of the wall jet model:

1. Collapse of axial mean and fluctuating velocities onto a single similarity profile characteristic of wall jets.
2. Agreement of the velocity decay and jet expansion with literature values.

These criteria require that the effect of tank curvature be negligible, and that in spite of the relatively complicated origin of the wall jet in a stirred tank, the expansion of the jet be linear.

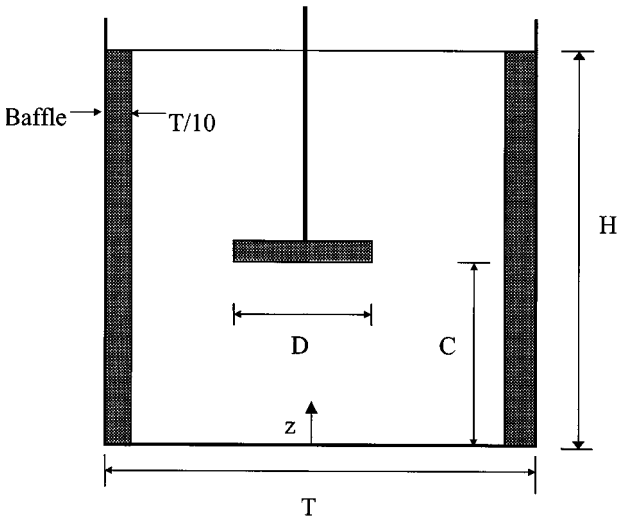

Figure 3a. Tank configuration (side view) and notation.

Similarity profile

For the flow to be considered a jet, the velocity profiles must collapse onto a single similarity profile as the jet proceeds upward in the tank. Figures 4a–4c show the collapsed similarity profiles for wall jets produced by the A310, HE-3, and PBT. The data in these figures were taken on Traverse A (shown in Figure 3b) at various axial positions. In the similarity profiles U_m is the local maximum velocity in each of the profiles, $z/T = 0$ at the bottom of the tank, and $\eta = 0$ at the

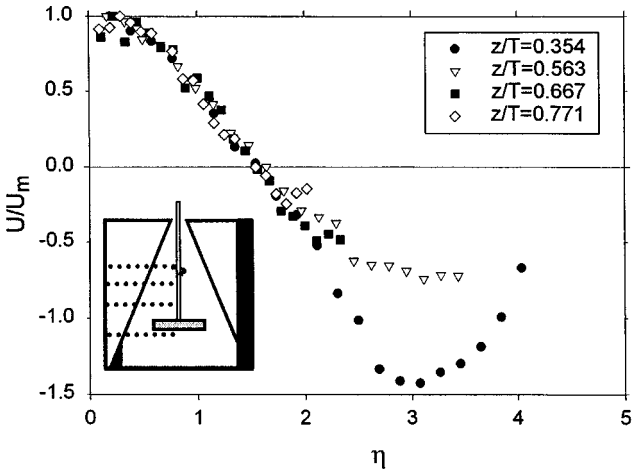

Figure 4a. Dimensionless axial velocity for the A310 impeller at $C/D = 0.68$ and $Re = 1.96\times10^5$.

Profile fits at $U/U_m = 0.5$ and at 1.0 by definition; similarity is maintained beyond the end of the jet model ($U/U_m = 0$), except for one traverse below the impeller ($z/T = 0.354$), where additional momentum is injected into the flow.

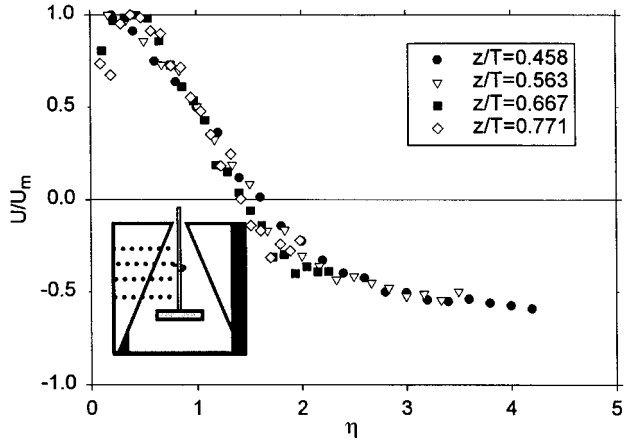

Figure 4b. Dimensionless axial velocity for the PBT impeller at $C/D = 0.4$ and $Re = 5.33 \times 10^4$.

Profiles match at $U/U_m = 0.5$ and 1.0 by definition; similarity is maintained beyond $U/U_m = 0$ for all profiles.

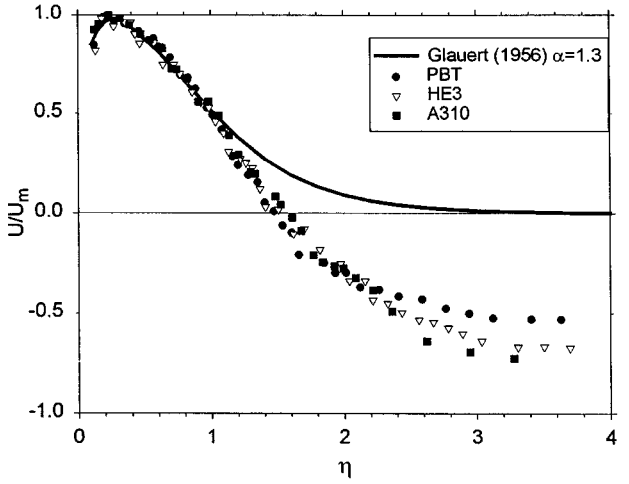

Figure 5. Axial velocity for three axial impellers vs. theoretical wall jet model.

The velocity matches Glauert's theory to $\eta = 1.2$, after which recirculation affects the profiles. Similarity between all three impellers is maintained up to $\eta = 2.3$.

tank wall. Given the similarity of the profiles it can be concluded that the first criterion for the flow to be considered a wall jet is attained, with the other criteria being jet expansion, jet decay, and turbulent similarity.

The similarity profiles from Figures 4a–4c were averaged and compared to a classic wall-jet similarity profile from Glauert (1956). Figure 5 compares the average velocity profiles for the three impellers to the classic wall-jet profile from Glauert's equations (1956; $\alpha = 1.3$). In Glauert's solution, alpha is a function of the dimensionless boundary-layer thickness. For this data set, alpha was determined using the location of the maximum velocity for each impeller in combination with Glauert's Figure 3. For all three cases, $\alpha = 1.3$. Because the outer layer of the jet is of greatest interest, the experiments focus on the profile from $U/U_m = 1$ to $U/U_m = 0$. The velocity profiles match Glauert's results very well up to $U/U_m \approx +0.4$. After this point, the results stray from the classic wall-jet results due to the recirculating flow in the tank. This is to be expected, since the wall jet in a stirred tank ends as a shear layer begins, whereas the classic wall-jet results were obtained using a free stream velocity of zero.

Perhaps even more useful than the agreement with established characteristics of wall jets is the fact that the wall-jet profiles collapse exactly for all three axial impellers. The exact match of the profiles from $U/U_m = 1$ to $U/U_m = -0.4$ is extremely useful for the modeling of these flows. This allows a complete characterization of the vertical circulation using only U_{core} and the decay of U_m for *all* axial impellers. The collapse of the profiles can be attributed to the continuity of shear stress at the interface between the two shear layers (the wall jet and the impeller suction). The viscosity in the two shear layers is the same, hence the slopes must be equal, which is what the data in Figures 4a–4c show.

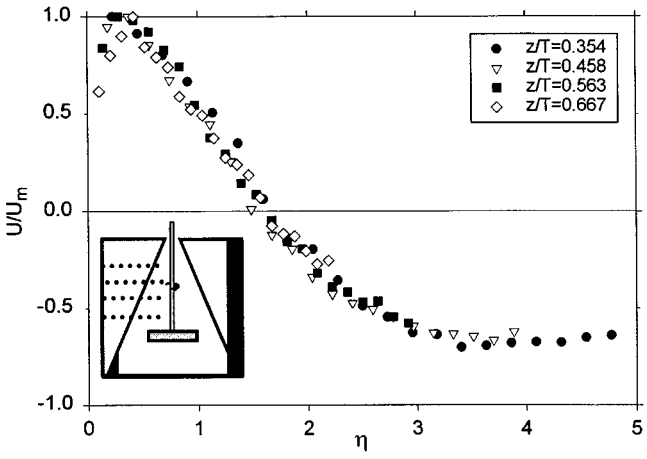

Figure 4c. Dimensionless axial velocity for the HE-3 impeller at $C/D = 0.5$ and $Re = 2.40 \times 10^4$.

Profiles match at $U/U_m = 0.5$ and 1.0 by definition; similarity is maintained beyond $U/U_m = 0$ for all profiles.

Jet decay

The size of the development zone and the velocity decay are examined next. Figures 6a–6c show the development and decay of the local maximum velocity in the wall jet for an A310, a PBT, and an HE-3 as a function of distance along the jet. Both axes use log scales in order to determine the exponent of the decay of U_m with z. The x-axis is the dimensionless distance (z/T) from the bottom of the tank and the y-axis is the dimensionless velocity (U_m/U_{core}): here U_{core} is the global maximum velocity.

Figure 6a shows the development zone for an A310 impeller. For this impeller, the development of the potential core extends from $z/T = 0$ to 0.28 as the radial flow impinges on the wall of the tank and is converted to vertical circulation. This is in good agreement with Fort et al. (1993), who showed that the height of the radial flow at the bottom of the tank is $z/T = 0.2$ for a 4-bladed airfoil impeller. After the

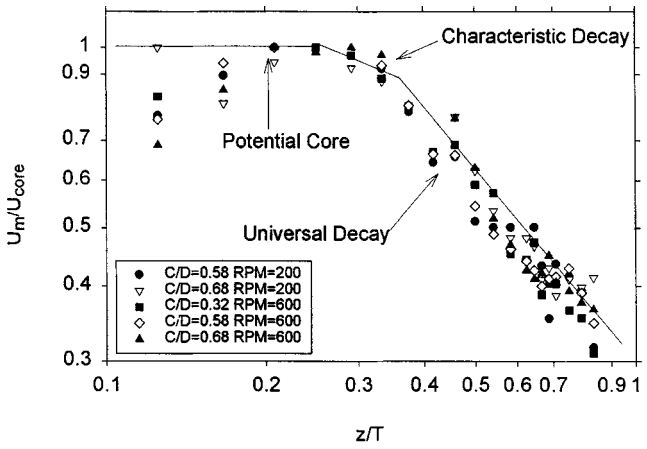

Figure 6a. Decay of maximum velocity for the wall jet driven by the A310 impeller for various dimensionless clearances (C/D) and rotational speeds.

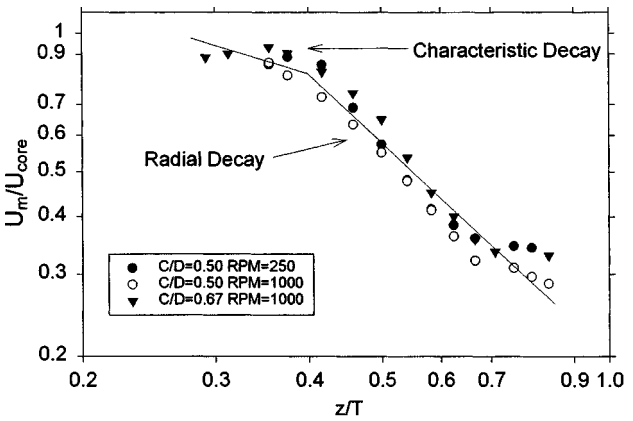

Figure 6c. Decay of maximum velocity for the wall jet driven by the HE-3 impeller for various dimensionless clearances (C/D) and rotational speeds.

impingement height, the jet needs another 0.10 z/T before it starts to decay. The development zone is similar for all three axial impellers, extending to $z/T = 0.28$, in spite of the fact that the off-bottom clearance varies from $0.32 < C/D < 0.68$.

Figures 6a–6c show the characteristic decay and the radial decay regions of the wall jet produced by an A310, PBT, and HE-3. The scatter in these figures is within experimental error. The slope of the velocity decay (exponent on z) was determined for each set of data using linear regression. The results, given in Table 3, show the range of slopes for both decay regions. The average slopes for the characteristic and radial decay are also given for all three impellers.

The characteristic decay zone has an average decay exponent of -0.48. The range of values for individual impellers is quite large due to the short length of this region (approximately $0.1\,z/T$), and the limited amount of data. The average values correspond to a square orifice geometry, for which characteristic decay exponents ranging from -0.16 to -0.61 (Padmanabham and Gowda, 1991) have been observed.

The decay of the local maximum velocity for a three-dimensional wall jet is proportional to the inverse of the distance traveled. The average slope in the radial decay region differs slightly from this theoretical exponent of -1. This is common for three-dimensional wall jets, as shown by Rajaratnam and Pani (1970), who found values ranging from -1.0 to -1.14; Swamy and Bandyopadhyay (1975), who found a value of -1.1; and Padmanabham and Gowda (1991), who found values in the literature ranging from -1.0 to -1.27. Launder and Rodi (1981) have shown that the friction along the wall leads to a more rapid decay due to the influence of the inner layer and the shear stress at the wall. Given this information, the average slope of -1.15 in the radial decay zone for axial impellers can be considered a very good match to the classic three-dimensional wall jet.

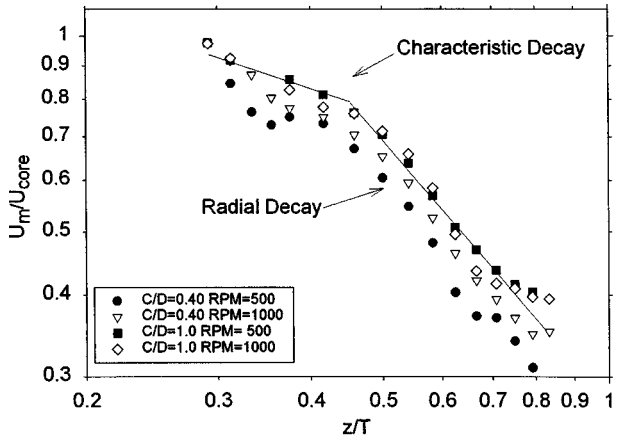

Figure 6b. Decay of maximum velocity for the wall jet driven by the PBT impeller for various dimensionless clearances (C/D) and rotational speeds.

Three-dimensional characteristics

The third dimension of the jet was examined by taking axial velocity measurements in the angular direction, as shown in Figure 3b, Traverse B. These profiles, reported in Figure 7, were examined to test for similarity and for a small boundary layer at the baffle wall. Beginning at $z/T = 0.67$, Traverse B shows evidence of a three-dimensional similarity profile. Similarity in the θ-direction appears later than similarity in the y-direction because of the continuity constraint near the bottom of the tank. The flow upward must match the flow from the impeller discharge, and the only upward flow is near the walls of the tank. To minimize the energy required to satisfy continuity, the flow spreads out in the theta direction. In spite of this angular distribution in the volumetric flow up to $z/T \approx 0.5$, the axial velocities terminate their upward climb at different points and the decay of U_m behaves like a three-dimensional jet from $z/T \approx 0.4$ (see Figure 6). In a jet formed by a ring source (that is, a two-dimensional jet), the velocities would all terminate at the same point and the decay of U_m would be proportional to $z^{-0.5}$ (Bittorf, 2000); hence, one

Table 3. Range and Average Decay Coefficient of Wall Jet for Axial Impellers

Impeller	Range of Slopes	Average Slope	Average Intercept	R^2 of the Average Slope
Characteristic Decay Zone				
A310	−0.27 to −0.86	−0.48	−0.31	0.76
PBT	−0.47 to −0.66	−0.59	−0.35	0.88
HE-3	−0.29 to −0.44	−0.30	−0.19	0.73
average		−0.49	−0.30	0.73
Radial Decay Zone				
A310	−0.95 to −1.12	−1.00	−0.54	0.97
PBT	−1.08 to −1.29	−1.13	−0.61	0.97
HE-3	−1.19 to −1.48	−1.30	−0.60	0.90
average		−1.15	−0.56	0.94

Table 4. Expansion Rate and Virtual Origin of Wall Jet in Stirred Tank

Experiment	Expansion ($\Delta b/\Delta z$)	Virtual Origin (mm)
PBT $D/T = 0.33$ $C/D = 0.40$	0.38	−20
A310 $D/T = 0.58$ $C/D = 0.68$	0.36	−16
HE-3 $D/T = 0.50$ $C/D = 0.50$	0.39	−29
Average for axial impellers	**0.38**	**−22**

can conclude that the wall jet driven by axial impellers is best modeled as a three-dimensional jet issuing from a point source.

Jet expansion and its originating position

Once it is established that the jet starts from a theoretical point source, the origin of the point source and the expansion of the jet can be determined. The virtual origin of the jet for each of the axial impellers is given in Table 4. The average virtual origin is located approximately one baffle width below the bottom of the tank, as shown in Figure 2. The expansion of the wall jet ($\Delta b/\Delta z$) is also given in Table 4: the half-width of the jet spreads at an average of 0.38, or 20°, in the y-direction. This agrees well with Bains (1985), who predicted a 20° spread for a three-dimensional wall jet along two perpendicular walls. The spread is dependent on the environment of the jet, because this environment determines the profile of the jet. Moving away from the baffle in the theta direction, the expansion of the jet driven by the PBT has a slope of 0.19, or 10.7°. Although it is not uncommon for the expansion of a jet to be different in the two cross-stream directions (Bains, 1985), the curvature of the tank and/or the swirling component of the flow can retard the spreading of the jet in a stirred tank. If this is the case, the jet would spread faster in a larger tank, where the curvature is not as significant. This aspect of the jet behavior requires further investigation.

Turbulent intensities

The final characteristic of the jet to be examined for similarity is the fluctuating velocities in the jet. The velocity fluctuations in the streamwise direction were measured and compared to those reported elsewhere. In general, fluctuating velocities take longer to develop a similarity profile than mean velocities (Padmanabham and Gowda, 1991; Swamy and Bandyopadhyay, 1975; and Newman et al., 1971). Figure 8 shows the RMS velocity (u') made dimensionless with the local maximum velocity (U_m) for the A310 impeller. It takes a distance of $z/T = 0.66$ from the bottom of the tank before the profiles start to show similarity. Similarity occurs at z/T

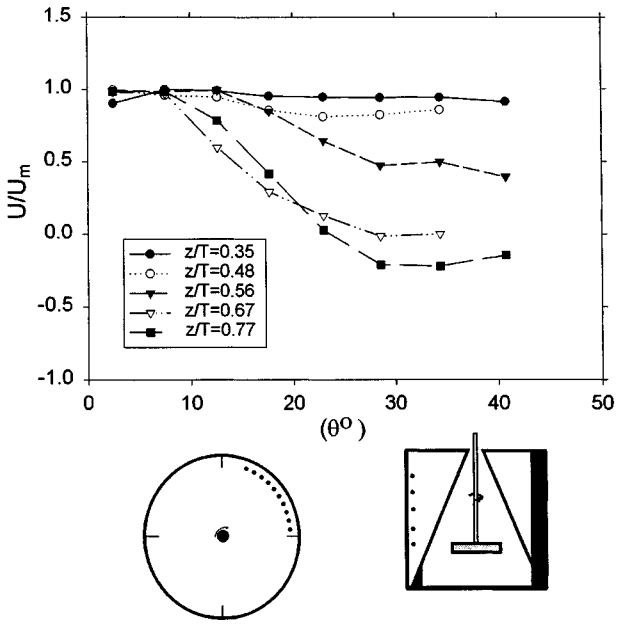

Figure 7. Velocity profiles along the wall of the tank (Traverse *B* in Figure 3b) for the PBT impeller at $C/D = 1$.

The jet develops a similarity profile in the θ-direction at a dimensionless height of $z/T = 0.67$.

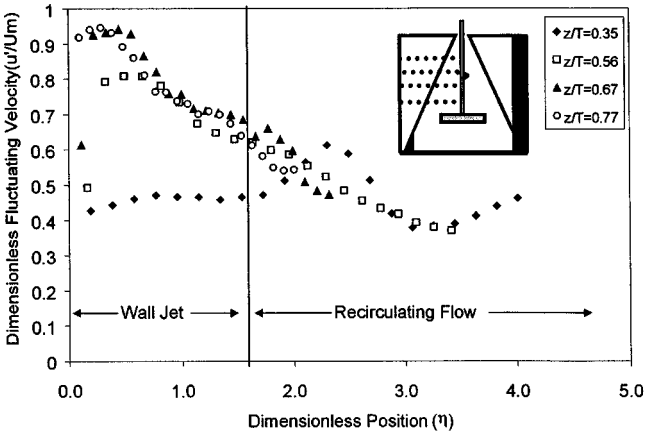

Figure 8. Turbulence in the three-dimensional wall jet produced by an A310 impeller ($D/T = 0.58$, $C/D = 0.68$, $N = 600$ rpm).

It takes a distance of $z/T = 0.67$ before fluctuating velocities show similarity.

$= 0.56$ for $\eta > 0.8$. This suggests that full similarity occurs between $z/T = 0.56$ and $z/T = 0.66$. The similarity of turbulent intensities satisfies the final criterion used to determine the existence of a three-dimensionl wall jet in stirred tanks agitated with axial impellers.

Conclusions

This study has shown that the vertical circulation along the baffle of a stirred tank agitated with an axial impeller forms a three-dimensional wall jet. Five major characteristics of the wall jet can be summarized from this work:

- The local maximum velocity decays inversely with the distance traveled ($U_m \propto z^{-1}$).
- The jet expansion in the y-direction is proportional to the distance traveled ($b \propto z$).
- The mean velocity profiles exhibit similarity beyond $z/T = 0.354$ in the y-direction (away from the wall), and beyond $z/T = 0.67$ in the angular direction (away from the baffle).
- The fluctuating velocity profiles exhibit similarity beyond $z/T = 0.67$ in the y-direction.
- Similarity is maintained in the recirculating flow beyond $U/U_m = 0$, up to $U/U_m = -0.4$ in the y-direction.

The strong similarity characteristics of the velocity profiles at the wall of the tank are somewhat surprising, given the complexity of the flow, but agree very well with jet theory. These results provide simplified models and an increased understanding of the characteristics of flow in a stirred tank. With the ability to approximate the flow at the wall with a jet and a potential core region, better models of solids distribution and averaged zone models of the tank may be possible. Finally, these results provide a set of meaningful test data for CFD validation.

Notation

b = distance to $U_m/2$, L
C = clearance, L
d_{nozzle} = nozzle diameter of the wall jet, L
D = impeller diameter, L
H = tank height $H = T$, L
N = impeller speed (t^{-1})
p = exponent in similarity solution
q = exponent in similarity solution
Re = Reynolds number (ND^2/ν)
T = tank diameter, L
r = radial coordinate
U_{core} = core velocity, $L \cdot t^{-1}$
U_{nozzle} = nozzle velocity, $L \cdot t^{-1}$
U = axial velocity component, $L \cdot t^{-1}$
U_m = local maximum velocity, $L \cdot t^{-1}$
u', v', w' = fluctuating velocity, $L \cdot t^{-1}$
V = y or r velocity component, $L \cdot t^{-1}$
W = x or θ velocity component $L \cdot t^{-1}$
x, y, z = Cartesian coordinates, L
y = distance from tank wall, L
z = axial coordinate, L

Greek letters

α = constant from Glauert (1956)
θ = tangential coordinate, deg
ν = kinematic viscosity, $L^2 \cdot t^{-1}$
η = dimensionless distance
ρ = density, $M \cdot L^{-3}$

Literature Cited

Abrahamsson, H., B. Johansson, and L. Fofdahl, "A Turbulent Plane Two-Dimensional Wall-Jet in a Quiescent Surrounding," *Eur. J. Mech., B/Fluies*, **13**, 533 (1994).

Bains, D. W., "Entrainment by a Buoyant Jet Flowing Along Vertical Walls," *J. Hydraul. Res.*, **23**, 221 (1985).

Bittorf, K. J., and S. M. Kresta, "Active Volume of Mean Circulation for Stirred Tanks Agitated with Axial Impellers," *Chem. Eng. Sci.*, **55**, 1325 (2000).

Bittorf, K. J., "The Application of Wall Jets in Stirred Tanks," PhD Thesis, University of Alberta (2000).

Bruha, O., I. Fort, and P. Smolka, "Phenomenon of Turbulent Macroinstabilities in Agitated Systems," *Collect. Czech. Chem. Commun.*, **60**, 85 (1995).

Eriksson, J. G., R. I. Karlsson, and J. Persson, "An Experimental Study of a Two-Dimensional Plane Turbulent Wall Jet," *Exp. Fluids*, **25**, 50 (1998).

Fort, I., "Flow and Turbulence in Vessels with Axial Impellers," *Mixing: Theory and Practice*, Vol. III, V. W. Uhl and J. B. Gray, eds., Academic Press, New York, p. 133 (1986).

Fort, I., M. Vozny, and T. Makovsky, "Flow and Turbulence in a Baffled System with Impeller with Inclined Blades," *ACTA Polytech.*, **33**, 31 (1993).

Gerodimos, G., and R. M. C. So, "Near-Wall Modeling of Plane Turbulent Wall Jets," *J. Fluids Eng.*, **119**, 304 (1997).

Glauert, M. B., "The Wall Jet," *J. Fluid Mech.*, **1**, 625 (1956).

Kresta, S. M., and P. E. Wood, "Prediction of the Three Dimensional Turbulent Flow in Stirred Tanks," *AIChE J.*, **37**, 448 (1991).

Kresta, S. M., "Boundary Conditions Required for the CFD Simulation of Flows in Stirred Tanks," *Advances in Fluid Mechanics: Multiphase Reactor and Polymerization System Hydrodynamics*, N. P. Cheremisinoff, ed., Gulf Publ., Houston, p. 297 (1996).

Launder, B. E., and W. Rodi, "The Turbulent Wall Jet," *Prog. Aerospace Sci.*, **19**, 81 (1981).

Newman, B. G., R. P. Patel, S. B. Savage, and H. K. Tjio, "Three-Dimensional Wall Jet Originating from a Circular Orifice," *Aero. Q.*, **23**, 188 (1972).

Padmanabham, G., and B. H. Gowda, "Mean and Turbulence Characteristics as a Class of Three-Dimensional Wall Jets—Part 1: Mean Flow Characteristics," *J. Fluids Eng.*, **113**, 620 (1991).

Per, P., L. Magnus, and J. Lennart, "Measurements of the Velocity Field Downstream of an Impeller," *J. Fluids Eng.*, **118**, 602 (1996).

Rajaratnam, N., and B. S. Pani, "Three-Dimensional Turbulent Wall Jets," Tech. Rep., Dept. of Civil Engineering, Univ. of Alberta, Edmonton, Alta., Canada (1970).

Rajaratnam, N., and B. S. Pani, "Three-Dimensional Wall Jets," *Proc. ASCE, J. Hydraulics Div.*, **100**, 69 (1974).

Rajaratnam, N., "Developments in Water Sciences, Turbulent Jets," Elsevier, New York (1976).

Roussinova, V., B. Grgic, and S. M. Kresta, "Study of Macro-Instabilities in Stirred Tanks Using a Velocity Decomposition Technique," *Chem. Eng. Res. Des.* (2000).

Schwarz, W. H., and W. P. Cosart, "The Two-Dimensional Wall-Jet," *J. Fluid Mech.*, **10**, 481 (1960).

Swamy, N. V., and P. Bandyopadhyay, "Mean and Turbulence Characteristics of Three-Dimensional Wall Jets," *J. Fluid Mech.*, **71**, 541 (1975).

Venas, B., H. Abrahamsson, P. A. Krogstad, and L. Lofdahl, "Plused Hot-Wire Measurements in Two and Three-Dimensional Wall Jets," *Exp. Fluids*, **27**, 210 (1999).

Zhou, G., and S. M. Kresta, "Distribution of Energy Between Convective and Turbulent Flow for Three Frequently Used Impellers," *Trans. Inst. Chem. Eng.*, **74**, 379 (1996).

Manuscript received August 2, 2000, and revision received Nov. 16, 2000.